Gradient-Elastic Tensor in Sodium Chloride and Sodium Bromide*

J. L. MARSH, JR.,† AND P. A. CASABELLA†
Interdisciplinary Materials Research Center, Rensselaer Polytechnic Institute, Troy, New York
(Received 18 May 1966; revised manuscript received 24 June 1966)

The effects of static elastic strain on the Nuclear Magnetic Resonance (NMR) spectra of NaCl and NaBr were used to determine the gradient elastic tensors for the ions in these crystals. The measured tensor components were compared with the results of a point-ion model to provide effective antishielding factors for the ions observed. The effective antishielding factors were found to be larger in the case of Na^{23} and smaller for Cl^{35} and Br^{79} than the corresponding theoretical antishielding factors. These discrepancies are explained by a consideration of first and second nearest-neighbor overlap effects.

INTRODUCTION

IN a strain-free cubic crystal, the local field gradients vanish at the nuclear sites because of the cubic symmetry of the lattice. It is possible to lower this symmetry and thus to produce observable quadrupole interactions in a variety of ways. The effects of strain on the quadrupole interaction in ionic crystals have interested many investigators since they were first studied by Watkins and Pound.[1,2] Several different techniques have been used to investigate the gradient-strain coupling in solids. They fall into three rough categories: static-elastic-strain experiments[3,4] plastic-deformation and mixed-crystal experiments[5,6]; and ultrasonic and relaxation experiments.[7–9] While each method has its shortcomings, the elastic-deformation technique was chosen because it is the most direct method, provided suitably perfect single crystals are available.

For sufficiently small strain, the change in field gradient at the nuclear site should be proportional to the ion displacements and thus expressible in terms of a tensor of fourth rank **S** connecting the field gradients with the elastic strains. It is easy to calculate the gradients produced by small displacements of a lattice composed of point ions. The ratio of the measured field gradients or corresponding **S** components to those predicted by the point-ion model is an effective antishielding factor β for the ion under study. In fact it would equal the usual theoretical Sternheimer antishielding factor $(1+\gamma)$ if the point-ion model was adequate for these highly ionic solids. Deviations of the observed effective antishielding values from the theoretical antishielding factors may be explained by a consideration of first-nearest-neighbor overlap for the sodium ion and first- and second-nearest-neighbor overlap effects for the chlorine and bromine ions. Aside from the information they provide about effective antishielding factors, the **S** tensor components are important in the study of acoustical NMR,[9] and for the investigation of defects by NMR.[10]

The approach which was chosen for this investigation was the following: (a) Elastically deform an oriented single crystal while monitoring the NMR spectra; (b) determine the field gradients from the changes in the NMR spectra caused by the quadrupole interaction; (c) use the field gradient to find the **S**-tensor components; (d) compare the **S** components with the point-ion model to get effective antishielding factors (β); and (e) compare the effective antishielding factors with the sum of the theoretical antishielding factor plus contributions under strain due to the central ion's overlap with its neighboring ions.

EXPERIMENTAL APPARATUS

The apparatus consisted of an aluminum-alloy low-pressure NMR cell and a Pound-Watkins marginal oscillator and lock-in system. All frequency measurements were made with a loosely coupled Hewlett-Packard frequency counter (1 part in 10^8 accuracy). The pressure cell consisted of a simple piston and cylinder assembly mounted in a vertical position between the pole pieces of an electromagnet. In order to

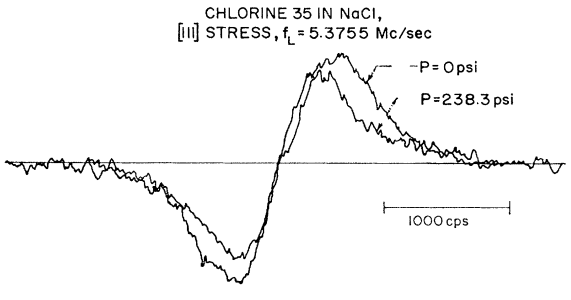

FIG. 1. Examples of strained and unstrained Cl^{35} NMR lines in NaCl. f_L is the Larmor frequency.

* This work was supported by the National Aeronautics and Space Administration. It is based upon the dissertation submitted by J. L. Marsh, Jr., in partial fulfillment of the requirements for the Ph.D. degree at Rensselaer Polytechnic Institute.

† Department of Physics.

[1] G. D. Watkins and R. V. Pound, Phys. Rev. **89**, 658 (1953).

[2] R. V. Pound, J. Phys. Chem. **57**, 743 (1953).

[3] R. G. Schulman, B. J. Wylunda, and P. W. Anderson, Phys. Rev. **107**, 953 (1957).

[4] V. V. Lemanov, Zh. Eksperim. i Teor. Fiz. **40**, 775 (1961) [English transl: Soviet Phys.—JETP **13**, 543 (1961)].

[5] H. Kawamura, E. Otsuka, and K. Ishiwatari, J. Phys. Soc. Japan **11**, 1064 (1956).

[6] Y. Fukai, J. Phys. Soc. Japan **19**, 175 (1964).

[7] M. Menes and D. I. Bolef, Phys. Rev. **109**, 218 (1958).

[8] E. F. Taylor and N. Bloembergen, Phys. Rev. **113**, 431 (1959).

[9] D. I. Bolef and R. K. Sundfors, Proc. IEEE **53**, 1574 (1965).

[10] O. Kanert, Phys. Status Solidi **7**, 791 (1964).

develop the desired pressures (up to 1000 psi) weights were hung on the end of a lever arm which pressed down on the top of the piston. To avoid non-uniaxial stress, the piston and cylinder were accurately machined and the surfaces contacting the sample were coated with a hard, nonconducting, arc-sprayed ceramic which could be diamond-polished. The samples were 1.5 cm long by 1.2 cm in diameter, cylindrical, single crystals, supplied by the Harshaw Chemical Company.

CALCULATION OF THE FIELD GRADIENT FROM THE RECORDED NMR SPECTRA

Typical recordings are shown in Fig. 1 for the Cl^{35} resonance in NaCl under [111] stress. Note the broadening of the resonance and reduction in recorded derivative maxima under elastic loading. The line returns to its original shape upon removal of the stress. To find the field gradient from recordings such as these one must relate the change in observed line shape to the first-order frequency shift of the satellites. This was done by the method of Schulman *et al.*[1] Thus it was assumed that elastic deformation produces only a shift of the satellites without any change in their shape, and that the central-limit theorem is valid. Then the independent contributions could be simply added to find the total second moment of the resonance line. On this basis one can write

$$\Delta\nu^2=\Delta\nu_0^2+k\Delta f^2 \tag{1}$$

or

$$\Delta f=(\Delta\nu^2-\Delta\nu_0^2)^{1/2}k^{-1/2}, \tag{1'}$$

where $\Delta\nu_0^2$ and $\Delta\nu^2$ are the second moments of the undeformed and deformed absorption lines, respectively; Δf is the first-order satellite frequency shift, and k is the satellite intensity relative to the total line intensity.

If it is further assumed that the stressed and unstressed lines have the same shape function; the splitting may be related to the derivative maxima of the NMR lines. The integrated intensity of an absorption line is proportional to the product of the derivative maximum and the second moment. Under elastic strain the integral intensity should not change. Thus for a fixed line shape

$$\Delta\nu^2=A_0\Delta\nu_0^2/A, \tag{2}$$

where A_0 and A are the unstressed and stressed derivative maxima, respectively. If Eq. (2) is substituted into Eq. (1'), the result is

$$\Delta f=(\Delta\nu_0^2/k)^{1/2}(A_0-A)^{1/2}A^{-1/2}. \tag{3}$$

In this work both Eqs. (1') and (3) were used to analyze the data and they agreed quite closely, except for the largest line splitting where only the second moment relation (1') was used. It is possible to measure A and A_0 more accurately than $\Delta\nu^2$, but the assumption of no change in the total line shape under stress is quite drastic.

The relative satellite intensity factors (k) were determined by plastically deforming sodium chloride samples until all the first-order sodium and chlorine satellites were wiped out by local lattice imperfections. The integrated intensities of the remaining central lines could then be used as standards for calibrating the other sodium and chlorine recordings for both alkali halides. k was found to be 0.6 for Na^{23} and Cl^{35} and zero for Br^{79}.

With sufficient stress applied in the [111] direction, it was possible to see the Cl^{35} satellites directly in NaCl samples. That is, they separated sufficiently from the central line to be observable as extra bumps on the resonances. An example of this is shown in Fig. 2.

Figure 3 is a graph of the satellite frequency splitting as a function of pressure for the Cl^{35} resonance in the NaCl [111] pressure experiments. The circled data points were determined by second-moment analysis. The triangles represent the directly observed splittings. The solid line is a least-squares fit through the origin with the slope $\Delta f/P=2.09\pm0.07$ cps/psi. The $\Delta f/P$ values for all the first-order experiments are shown in Table I.

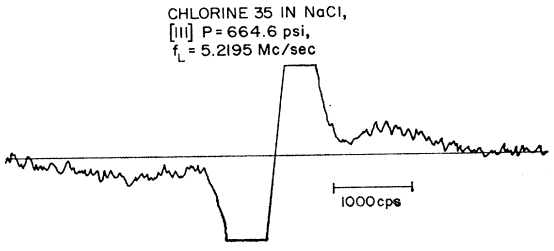

FIG. 2. Direct observation of Cl^{35} first-order satellites in NaCl under [111] stress. The frequency splitting of one satellite from the central line is approximately 1200 cps for the stress shown.

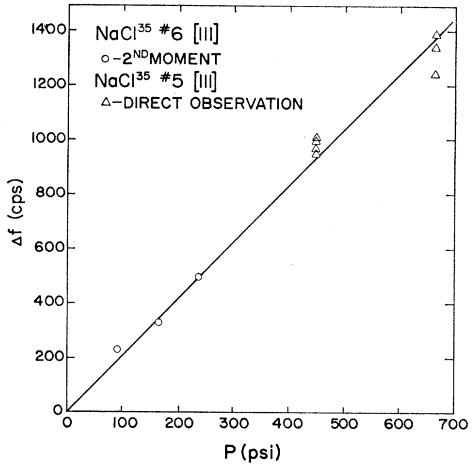

FIG. 3. The first-order-satellite frequency splitting (Δf) as a function of [111] stress (P) for the Cl^{35} resonance in NaCl.

TABLE I. The experimental gradient-strain-tensor components (S_{11} and S_{44}) for the nuclei studied. The data on first-order-satellite frequency splitting versus applied pressure ($\Delta f/P$) and certain previous values of S_{11} are also shown.

Nucleus	Crystal	$\Delta f/P$ (cps cm²/dyn) (×10)	S_{11}(cgs esu) (×10)	S_{44}(cgs esu) (×10¹⁵)	Previous data ($S_{11}\times10^{15}$)
Na^{23}	NaCl [100]	1.29	2.60 ±15%	···	1.1–1.3[a], 2.0[b], 2.73[c] erf 2 ±15% ±25%
Na^{23}	NaCl [111]	1.04		1.09 ±10%	0.55[b] (S_{44}) ±15%
Na^{23}	NaBr [100]	1.52	2.44 ±30%		2.42[c] ±25%
Na^{23}	NaBr [111]	1.02		0.824 ±20	
Cl^{35}	NaCl [100]	1.29	3.29 ±20%		2.3[a] erf 2
Br^{79}	NaBr [100]	Not observed			25.3[c] ±25%
Br^{79}	NaBr [111]			6.73 ±30%	

[a] Reference 8.
[b] Reference 4.
[c] Reference 6.

The first-order frequency splitting (Δf) of the Na and Cl satellites ($I=\frac{3}{2}$) is given by

$$\Delta f=\pm(eQ/2h)\phi_{nn}, \tag{4}$$

where eQ is the quadrupole moment of the nucleus and ϕ_{nn} is the field-gradient component in the direction of the static magnetic field. This relation is used to find ϕ_{nn} as a function of pressure from the frequency-splitting pressure data.

The second-order shift of the Br^{79} central line was measured for NaBr [111] specimen. The observed shift was 47.5±14 cps for a 1033 psi load. The Larmor frequency was 5.737 Mc/sec. The usual second-order formula was used to find ϕ_{nn} in terms of the shift.

ELECTRIC FIELD GRADIENT ELASTIC STRAIN TENSOR, S

The concept of the **S** tensor was first introduced by Taylor and Bloembergen[8] in their ultrasonic study of the Na and Cl resonances in NaCl. It is a tensor of the fourth rank, connecting the change in field gradient with the lattice strains

$$\phi_{\mu\nu}-\phi_{\mu\nu}{}^0=\sum_{k,\lambda} S_{\mu\nu k\lambda}\epsilon_{k\lambda}, \tag{5}$$

where ϕ^0 is the unstrained field-gradient tensor (zero for a strain-free cubic crystal), ϕ are the gradients observed under strain, and ϵ is the strain tensor. It may be easily shown[3] that, for the cubic point-group symmetry of the lattice, only three independent components of **S** exist, i.e., $S_{11}=S_{xxxx}$; $S_{12}=S_{xxyy}$; and $S_{44}=S_{yzyz}$.

The field-gradient components appear in the quadrupole Hamiltonian in such a fashion[11] that only two combinations of the **S** components may be observed, that is, $S_{11}-S_{12}$ and S_{44}. In order to be consistent with most previous authors, we fix the ratio of S_{11} and S_{12} such that the unobservable trace of the field-gradient tensor vanishes, and then only two components of **S** remain, S_{11} and S_{44}.

In terms of the elastic compliances (**s**) and the applied stress (**X**), the field gradients may be written as follows:

$$\phi_{xx}=S_{11}(s_{11}-s_{12})[X_{xx}-\tfrac{1}{2}(X_{yy}+X_{zz})], \tag{6}$$
$$\phi_{xy}=S_{44}s_{44}X_{xy}; \text{ cyclic in } x, y, z \text{ (cubic axes)}.$$

In these experiments, the direction of applied stress was perpendicular to the direction of the magnetic field. The stress was applied along the [001] or [111] axial directions of two sets of cylindrical specimens. A stress (P) applied along the [001] axis produces the following field-gradient component in the direction of the magnetic field[4]:

$$\phi_{nn}=-\tfrac{1}{2}S_{11}(s_{11}-s_{12})P. \tag{7}$$

The same stress (P) along the [111] axis produces

$$\phi_{nn}=-S_{44}s_{44}P. \tag{8}$$

In both Eqs. (6) and (7), ϕ_{nn} is independent of rotations about the applied stress. Substitution of Eq. 4 (in the case of Br, the appropriate second-order relation) into Eqs. (7) or (8) will give expressions for S_{11} and S_{44} in terms of the frequency splittings or shifts.

The $\Delta f/P$ and resulting S_{11} and S_{44} values are listed in Table I. Also included are several other values of **S** from the literature. Since the Cl^{35} [111] satellites were observed directly, the Cl^{35} S_{44} value is considerably more accurate than the other measurements. The relative signs of S_{11} and S_{44} were not determined in these experiments, but could be obtained from rotation experiments. They are assumed to have opposite signs on the basis of the point-ion model's prediction and most other independent measurements.

[11] R. J. Harrison and P. L. Sagalyn, Phys. Rev. **128**, 1630 (1962).

TABLE II. The effective antishielding factors (β_{11} and β_{44}) for the nuclei studied. The range of values of the published theoretical antishielding factors $(1+\gamma)$ for the appropriate ions is also shown.

Nucleus	Crystal	β_{11}	β_{44}	Theoretical $(1+\gamma)$
Na^{23}	NaCl	10.36	8.68	5.1–5.5
Na^{23}	NaBr	11.56	7.82	5.1–5.5
Cl^{35}	NaCl	13.11	32.02	28–88
Br^{79}	NaBr		63.8	100, 124

EFFECTIVE POINT-ION ANTISHIELDING FACTORS

The pure ionic or point-ion model is one in which the alkali halide is considered to be an array of nonoverlapping, spherically symmetric ions. The local field gradient is just the sum of the field gradients due to point charges located on the lattice sites. For a binary crystal only a single parameter is required to completely specify the field gradients produced by a strain. The result[12] is

$$S_{11}=-2S_{44}=\pm 11.8e/a^3 \tag{9}$$

where a is the nearest-neighbor distance and the sign of S_{11} is the same as that of the ion under consideration.

As was mentioned in the introduction, the effective antishielding factors, β_{11} and β_{44}, are equal to the ratio of the corresponding experimental **S** values to the point-ion **S** values given by Eq. (9). The calculated β values are shown in Table II.

The experimental values of β which are shown in Table II are larger in the case of the sodium ions and smaller for the halogen ions than the corresponding free-ion theoretical values $(1+\gamma)$. This problem has appeared in nearly all measurements which give information on antishielding in ionic crystals. Previous attempts to explain the disagreement between the experimental and theoretical factors may be separated into two categories: (a) modification of the free-ion antishielding factor when the ions are incorporated into a solid, and (b) improved calculation of contributions to the electric field gradients.

Burns and Wikner[13] have used the first approach and find a reduction of the antishielding factors of large ions by assuming a contraction of wave functions in crystals. While this effect is certainly important, it is not able to account for the sodium-ion data because the contraction of wave functions will reduce $(1+\gamma)$ of both positive and negative ions.

The second approach has been used by other investigators who considered the effects of covalency and/or overlapping on the field gradients.[6,14–16] When an alkali halide is strained, the outer p-electron distribution will become distorted from cubic symmetry. This distortion is caused by changes in covalency and overlap and will produce field gradients at the nuclear sites.

Fukai[6] has used the combined effects of nearest-neighbor overlap and covalent charge transfer to explain his antishielding data obtained from mixed-crystal experiments. Unfortunately, because many of the required overlap and covalency parameters were not available, he had to estimate them. Yamagata[16] found that halogen-halogen second-nearest-neighbor overlaps contribute more to the Cl chemical shifts of LiCl and NaCl than do the nearest-neighbor overlaps. His results also indicate that covalency effects are quite small in alkali halides.

OVERLAP MODEL

In this model we have extended the overlap calculations of Kondo and Yamashita[15] or Fukai[6] to include the contributions of second-nearest-neighbor overlap to the effective antishielding factors β_{11} and β_{44}. They use the method of symmetric orthogonalization[17] to construct an orthogonal set of wave functions from the atomic orbitals of the free ions in the ground state. The point of interest is that the overlap integrals between atomic wave functions on different ions constitute a measure of the distortion of the outer p-electron distribution.

Fukai's result[6] for the electronic overlap contribution to the component of the field gradient in the direction of the magnetic field is given by

$$\phi_{nn}{}^{e}=-6/5e(1+R)\langle r^{-3}\rangle \Sigma_i D_i(\alpha_i{}^2-\tfrac{1}{3}), \tag{10a}$$

where

$$R=\langle \gamma(r) r^{-3}\rangle/\langle r^{-3}\rangle, \tag{10b}$$

$\langle r^{-3}\rangle$ is the expectation value of r^{-3} for a p orbital of the atom at the site where the field gradient is being evaluated, and α_i is the direction cosine between the magnetic field direction and the position vector of the ith neighboring ion. Also

$$D_i=2\,\Sigma_j\,|\Omega_{ij}|^2 \tag{10c}$$

and

$$\Omega_{ij}=\int \psi_i{}^{0*}(r)\psi_j(r)d\tau, \tag{10d}$$

where $\psi_i{}^0$ is a p orbital of the atom at the site where the field gradient is being evaluated and is directed toward the ith neighboring ion. ψ_j is the jth orbital of the ith ion, so the summation in Eq. (10c) is over the orbitals of the ith neighboring ion. The summation in Eq. (10a) is then a summation over neighboring ions.

The value of $\phi_{nn}{}^{e}$ given by Eq. (10a) vanishes for a site with cubic symmetry but will be nonzero if the lattice is strained. Fukai[6] shows how the electronic contributions to S_{11} can be obtained from Eq. (10a) by

[12] M. H. Cohen and F. Reif, in *Solid State Physics*, edited by F. Seitz and D. Turnbull (Academic Press Inc., New York, 1957), Vol. 5, p. 353.
[13] G. Burns and E. G. Wikner, Phys. Rev. **121**, 155 (1961).
[14] K. Yosida and T. Moriya, J. Phys. Soc. Japan **11**, 33 (1956).
[15] J. Kondo and J. Yamashita, J. Phys. Chem. Solids **10**, 245 (1959).
[16] Y. Yamagata, J. Phys. Soc. Japan **19**, 1 (1964).
[17] P. O. Löwdin, Advan. Phys. **5**, 1 (1956).

TABLE III. The values used in calculating the effective antishielding factors (β_{11} and β_{44}) for the nuclei shown by means of the point-ion-plus-overlap model. The subscripts (1 and 2) on ρ and D refer to the first- and second-nearest-neighbor overlaps, respectively. In this table γ is the antishielding factor, a is the lattice parameter, a/ρ the radial factor in an exponential approximation to the overlap integral (D), R is the antishielding factor for gradients produced by the local ion's outermost electrons, and $\langle 1/r^3\rangle$ is the mean value of r^{-3} over an outermost p orbital. (a.u.=atomic units.)

Nucleus	Crystal	$1+\gamma$	a(Å)	a^3(10^2a.u.)	a/ρ_1	$D_1\times10^3$	a/ρ_2	$D_2\times10^3$	R	$\langle 1/r^3\rangle$ (a.u.)
Na^{23}	NaCl	5.5[a]	2.820	1.515	8.36[b]	2.62[b]			0	16[c]
Na^{23}	NaBr	5.5[a]	2.989	1.804	8.25[d]	2.76[d]			0	16[c]
Cl^{35}	NaCl	28.04[e]	2.820	1.515	7.93[c]	7.56[c]	5.49[d]	13.21[d]	0.4[f]	5.71[b]
Br^{79}	NaBr	(60)[g]	2.989	1.804	8.04[d]	6.69[d]	5.44[d]	16.99[d]	0	(10)[g]

[a] R. E. Watson and A. O. Freeman, Phys. Rev. **131**, 250 (1963).
[b] Reference 15.
[c] Reference 16.
[d] Calculated from overlap data given in Ref. 18.
[e] Reference 13.
[f] R. M. Sternheimer, Phys. Rev. **105**, 158 (1957).
[g] Estimates based on the corresponding quantities used for Cl^-.

calculating the component of the field gradient in the [001] direction caused by the strain ϵ_{zz}. Similarly, to find the electronic contributions to S_{44}, the component of the electric field gradient in the [110] direction due to the strain ϵ_{xy}, must be calculated.

In order to carry out these calculations the dependence of D_i on R_i, the distance to the ith neighbor is approximated by the form

$$D_i=D_i(0)\exp(-R_i/\rho_i). \tag{11}$$

The values of D_i and ρ_i are the same for all of the nearest neighbors in the unstrained crystal and will be denoted by D_1 and ρ_1. Similarly, the values for the second-nearest neighbors are D_2 and ρ_2.

When these calculations are carried out including overlap terms out to second-nearest neighbors, the results obtained for the overlap contribution to S_{11} and S_{44} are

$$\begin{aligned} S_{11}{}^e&=8/5e(1+R)\langle r^{-3}\rangle[(a/\rho_1)D_1+(a/\sqrt{2}\rho_2-3)D_2]\\ S_{44}{}^e&=-12/5e(1+R)\langle r^{-3}\rangle[D_1+(1-a/\sqrt{2}\rho_2)D_2]. \end{aligned} \tag{12}$$

TABLE IV. The contributions of the overlap model to the effective antishielding factors (β_{11} and β_{44}). The experimental values shown are to be compared with the sum of the point-ion term $(1+\gamma)$ plus the overlap terms, D_1 (first-nearest neighbors) and D_2 (second-nearest neighbor).

	Experiment	Model	Point ions $(1+\gamma)$	$+D_1$	$+D_2$
Na^{23} in NaCl					
β_{11}	10.36	12.68	5.5	+7.18	
β_{44}	8.68	7.84	5.5	+2.34	
Na^{23} in NaBr					
β_{11}	11.56	14.41	5.5	+8.91	
β_{44}	7.82	8.74	5.5	+3.24	
Cl^{35} in NaCl					
β_{11}	13.11	16.29	28.04	−9.83	−1.92
β_{44}	32.02	43.09	28.04	−3.72	+18.77
Br^{79} in NaBr					
β_{11}	Not observed	43.42	60.0	−13.12	−3.16
β_{44}	63.8	91.0	60.0	−5.0	+36.0

The corresponding ionic contributions to S_{11} and S_{44} are obtained by multiplying the values of Eq. (9) by $(1+\gamma)$ and are given by

$$\begin{aligned} S_{11}{}^I&=\pm(11.8e/a^3)(1+\gamma)\\ S_{44}{}^I&=+(5.9e/a^3)(1+\gamma). \end{aligned} \tag{13}$$

The complete expressions for S_{11} and S_{44} can then be obtained by adding Eqs. (12) and (13). When these resulting values are divided by the point-ion values of S_{11} and S_{44} given in Eq. (9), the following expressions for β_{11} and β_{44} are obtained:

$$\begin{aligned} \beta_{11}&=(1+\gamma)\pm\frac{8}{59}(1+R)a^3\langle r^{-3}\rangle\\ &\quad\times\left[\frac{a}{\rho_1}D_1+\left(\frac{a}{\sqrt{2}\rho_2}-3\right)D_2\right],\\ \beta_{44}&=(1+\gamma)\pm\frac{120}{295}(1+R)a^3\langle r^{-3}\rangle\\ &\quad\times\left[D_1+\left(1-\frac{a}{\sqrt{2}\rho_2}\right)D_2\right]. \end{aligned} \tag{14}$$

Here the upper sign is for positive ions and the lower for negative ions.

The various parameters used to calculate β_{11} and β_{44} are shown in Table III. The contributions of $(1+\gamma)$, D_1, and D_2 to the β's are shown in Table IV, along with the experimental values of β. No D_2 contributions to the sodium-ion β values are listed because of the vanishingly small sodium-sodium overlap in these crystals. On the other hand, the large halogen-halogen overlap results in values of D_2 larger than those of D_1 for the halogen ions. The experimental- and overlap-model values of β agree quite well for the sodium ions, and the halogen-ion β values are in fair agreement, considering the accuracy of the experimental data. How-

ever, the latter agreement is partially dependent on the halogen-ion antishielding factors which were used.

Yamagata's[16] chlorine-chlorine overlap function is quite different from Hafemeister and Flygare's function.[18] Although the latter's overlap data were used in this calculation, Yamagata's function provides very close agreement with the most accurately measured β value, β_{44} for Cl. Hafemeister and Flygare's data were used because they had included the effect of σ-σ overlap in their evaluation of the chlorine-chlorine overlap.

[18] D. W. Hafemeister and W. H. Flygare, J. Chem. Phys. 43, 795 (1965).

CONCLUSIONS

It is apparent from this investigation and the bulk of earlier data that the point-ion model is not able to satisfactorily explain the **S**-tensor components or corresponding effective-antishielding factors which are observed in ionic solids. More detailed calculations of the electric field gradients in ionic solids are required. Reasonable agreement between the theoretical and experimental antishielding factors is obtained by including the effects of overlap with the first- and second-nearest-neighbor ions. The addition of pure covalent effects does not appear to be required in order to explain the results.

PHYSICAL REVIEW VOLUME 150, NUMBER 2 14 OCTOBER 1966

Radiation-Induced Expansion and Increase in Refractive Index of Magnesium Oxide; Evidence for the *F* Center*

WILLIAM PRIMAK AND JAGDISH LUTHRA†‡
Argonne National Laboratory, Argonne, Illinois
(Received 16 February 1966)

Magnesium oxide single-crystal fragments bombarded with H^+, D^+, and He^+ at several energies between 0.14 and 4 MeV were examined polarimetrically. The dilatation was determined from photoelastic measurements (order of magnitude 0.01), and an increase in refractive index (despite a concomitant decrease in density) was inferred from an interference effect noted in the polarimeter. The depth of the radiation-induced dilatation for the 0.14-MeV ions was determined by an etching procedure. The increase in refractive index was confirmed interferometrically for specimens bombarded with 40-MeV He^+, and also the dispersion of the change in refractive index was measured for the visible region. Anomalous dispersion caused by a small absorption band in the visible region was found, but most of the refractive index change was associated with a very large band in the ultraviolet. On thermal annealing the refractive-index increase vanished at ~450°C, but the dilatation remained until much higher temperatures were reached. From the refractive-index change and its dispersion, the wavelength of the ultraviolet absorption peak (~0.26 μ) and the associated number of color centers (multiplied by their oscillator strength) were calculated. Thus the absorption was determined despite impurity absorption which prevented its direct observation. From a comparison with the annealing behavior reported by others for the magnetic resonance signal identified as the *F* center, it is concluded that the optical absorption band is caused by the *F* center. It is shown that the expansion can be accounted for largely by vacancies which were generated during ion bombardment and which have formed *F* centers. Thus the magnesium oxide behaves very much like the alkali halides, except that in the case of the alkali halides vacancies may be introduced by ionization and on annealing may vanish with the centers, whereas in the case of magnesium oxide corpuscular radiation is required to produce the vacancies and on annealing may remain even when the color centers have vanished.

INTRODUCTION

INVESTIGATIONS of the radiation effects in magnesium oxide have for the most part arisen from an interest in its structural properties (e.g., dimensional stability, mechanical properties) or from an interest in color centers, particularly in hopes of finding a system analogous to that found in alkali halides. Magnesium oxide has proven a particularly difficult material in many investigations because of the high impurity concentration and the poor quality of available crystals. The present work was begun as an investigation of the expansion produced by low-energy ion bombardment, a subject apparently hitherto uninvestigated. It was discovered that the expansion and the color-center phenomena were simply and directly related in a manner (hitherto unknown) much like that known for the alkali halides. A brief summary of research in these areas follows, although little of it was pertinent to the start of our investigation.

The effect of combined corpuscular and ionizing

* Based on work performed under the auspices of the U. S. Atomic Energy Commission.
† Participant, Institute of Nuclear Science and Engineering, Argonne National Laboratory, as International Atomic Energy Agency Fellow, 1963–1964.
‡ Permanent address: Atomic Energy Establishment, Trombay, Bombay, India.